Canadian Conference - Pacific Conference on Earthquake Engineering 2023
Vancouver, British Columbia
June 25th – June 30th, 2023

New Hazard Models for Central Asia: Preliminary Results in Kyrgyzstan

Carlos Herrera[1*], Tuna Onur[2,3], Rengin Gok[4,5], Anna Berezina[6]

[1]Senior Seismologist, Onur Seemann Consulting, Inc., Victoria, BC, Canada
[2]Principal, Onur Seemann Consulting, Inc., Victoria, BC, Canada
[3]Adjunct Professor, Department of Civil Engineering, University of Victoria, Victoria, BC, Canada
[4]Staff Scientist, Lawrence Livermore National Laboratory, Livermore, CA, USA
[5]Technical Advisor, National Nuclear Security Administration, U.S. Department of Energy, Washington, DC, USA
[6]Chief of the National Data Center, Institute of Seismology, National Academy of Science of Kyrgyz Republic, Bishkek, Kyrgyzstan
[*]carlos@onurseemann.com (Corresponding Author)

ABSTRACT

In this paper we present a probabilistic seismic hazard assessment (PSHA) and results for Kyrgyzstan. These PSHA results were obtained through new hazard models that were developed for Central Asia as part of a recently concluded project, based on a larger and improved earthquake catalogue for the region. Area sources were used to account for diffuse seismicity, while fault sources characterize larger magnitude earthquakes occurring on known active faults. Ground motion models (GMM) developed from global strong motion databases were used to characterize the ground motion component. Seismic hazard in Kyrgyzstan is solely associated with shallow earthquakes within the continental crust. Results in some of the major cities show that nearby seismic sources (within 40 km) dominate the contribution to hazard. The smaller seismicity has a particularly important contribution to hazard at short periods, which diminishes at longer periods, where active faults start dominating the hazard in the larger magnitude range. This is the case observed in Bishkek, the capital of Kyrgyzstan. The seismic hazard in other cities like Karakol and Osh is mostly associated to nearby faults, mainly due to their large geologic slip rates. The region around Naryn exhibits smaller earthquake occurrence rates and faults with lower slip rates, resulting in lower spectral acceleration values compared with the other cities.

Keywords: Earthquake catalog, ground motions, hazard assessment, Central Asia, Kyrgyzstan

INTRODUCTION

With the goal of improving seismic hazard assessments in Kyrgyzstan, Kazakhstan, and Tajikistan, a major collaborative project led by the Lawrence Livermore National Laboratory was carried out for the region, involving local and international participants. The project started with the compilation of new earthquake detections from local sources in Central Asia, following with a location procedure using the available wave arrival times [1]. Then, non-tectonic events were removed from the catalogue and magnitudes were harmonized to Mw [2]. This resulted in an improved earthquake catalogue between 1900 and 2017 that contains nearly 450,000 earthquakes, which is roughly nine times the number of earthquakes included in the event catalogue of the International Seismological Centre [3] for the region.

Prior to the development of seismic hazard models for PSHA, [2] carried out a completeness analysis on the earthquake catalogue. This analysis defines magnitude ranges that vary temporally, where all the earthquakes within each magnitude range are effectively reported. The set of earthquakes outside of the range is not complete, and therefore it is filtered out from the catalogue. Considering the variations in earthquake detection capabilities over time, a completeness magnitude was defined for different time intervals, starting from Mw $\geq$ 5.3 in the early 1900's to Mw $\geq$ 3.2 in the recent decades. This resulted in a "complete" earthquake catalogue for Central Asia that can be used for PSHA applications.

This paper presents the development and associated results of the seismic hazard models for Central Asia, with particular focus on Kyrgyzstan. Seismic source characterization was carried out using the complete earthquake catalogue of Central Asia mentioned earlier [2], as well as geologic information on known active faults. The ground motion component was characterized using a set of GMMs that were deemed appropriate for the tectonic structure of the region. PSHA results from these models are shown in terms of hazard maps, uniform hazard spectra (UHS), and hazard deaggregations that depict the contribution to hazard of the seismic sources (in terms of magnitude-distance pairs) at a particular location.

PSHA MODEL DEVELOPMENT

To better address modeling uncertainty in PSHA, two models were formulated for Central Asia: a merged model and an alternate model. For the former, local experts from each country developed a national hazard model for their respective territory, delineating their own seismic sources and selecting the associated GMM logic trees. The seismic sources of these three national hazard models were harmonized at their borders to allow for a posterior merge. Therefore, the merged model is a single hazard model that combines the individually developed seismic sources and GMM logic trees of the three national hazard models, keeping the original formulation intended by the local experts for each of their territories. At the same time, the alternate model was developed by international experts for the entire region of Central Asia. In this model, the GMM logic tree includes sets of GMMs for each tectonic regime, but they do not change from country to country, as in the merged model.

Seismic source characterization

The seismic source component of the models was formulated using both area sources and fault sources. Area sources are polygons that account for the diffuse seismicity within their areas that cannot be associated to specific well-characterized active faults. These polygons are delineated following the seismicity patterns shown in the “complete” catalogue, tectonic features, and lineaments of known fault systems. Seismicity within the area sources is assumed to be homogeneous within its boundaries. Fault sources were delineated following the mapped strikes of active faults and the current knowledge of their geometry, slip kinematics, and geological slip rate. When combined in a hazard model, area sources generally contribute to the hazard associated with earthquakes of smaller magnitudes, while fault sources account for the hazard of larger earthquakes.

Starting at Mw 4.5 as minimum magnitude for hazard analysis purposes, the observed cumulative annual rate of earthquakes within each area source was modeled using a bounded Gutenberg-Richter relationship, which decreases asymptotically towards a maximum magnitude. If no faults are overlapping with the area source, the maximum magnitude was defined based on the largest observed earthquakes, physical and tectonic considerations appropriate for the region, and the polygon size, which sets the physical bounds of a hypothetical maximum rupture length that would fit within the polygon. Conversely, if a fault overlaps with the area source, the maximum magnitude of the area source was set as Mw 6.6, and the hazard of larger earthquakes was accounted for by the fault (see examples in Figure 1). This avoids double counting hazard when seismic sources are overlapping. This formulation was followed in both, the Kyrgyzstan national hazard model and the alternate model.

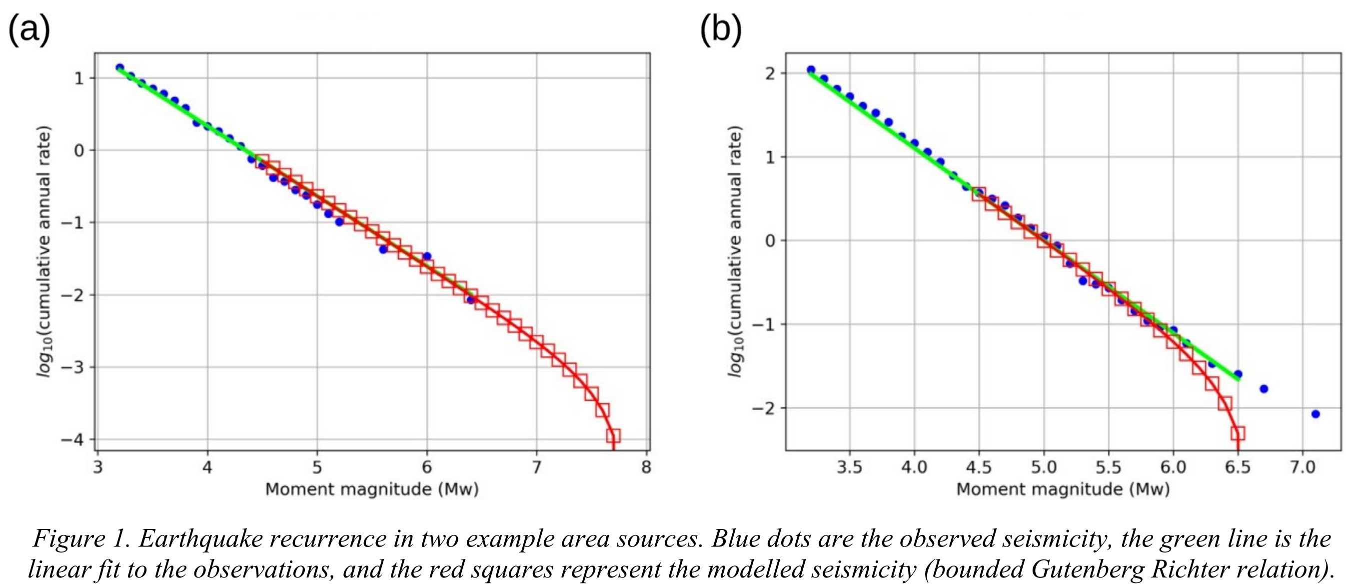

Figure 1. Earthquake recurrence in two example area sources. Blue dots are the observed seismicity, the green line is the linear fit to the observations, and the red squares represent the modelled seismicity (bounded Gutenberg Richter relation). (a) Area source without a fault source overlapping it. (b) Area source with an overlapping fault source. Despite the observed samples at larger Mw, the threshold for the modeled seismicity was set at Mw 6.6 (last sample trimmed out for being too small), since larger earthquakes are accounted for by the fault source.

Significant earthquake occurrence within the continental crust is observed in Kyrgyzstan and its nearby territories. Therefore, its area sources and their associated seismic recurrence were formulated using these earthquakes (Figure 2), as well as the main physiographic trends of its mountainous geography. The existence of numerous mountain ranges in Kyrgyzstan is associated with a significant number of crustal active faults across its territory. Most of these faults are oriented east-west (following the directions of the northern Pamirs and Tien Shan mountain ranges) and have reverse faulting mechanisms, except for the Talas-Fergana fault system, which is oriented NW-SE in western Kyrgyzstan and has a strike-slip mechanism. These faults have been well studied by local experts, with direct field observations of geometries, kinematics, and geological slip rates for most of them. The national hazard map of Kyrgyzstan features 97 faults within its territory, while the alternate model only includes the most relevant and well-studied faults (Figure 2), modelling the rest of the seismicity with area sources.

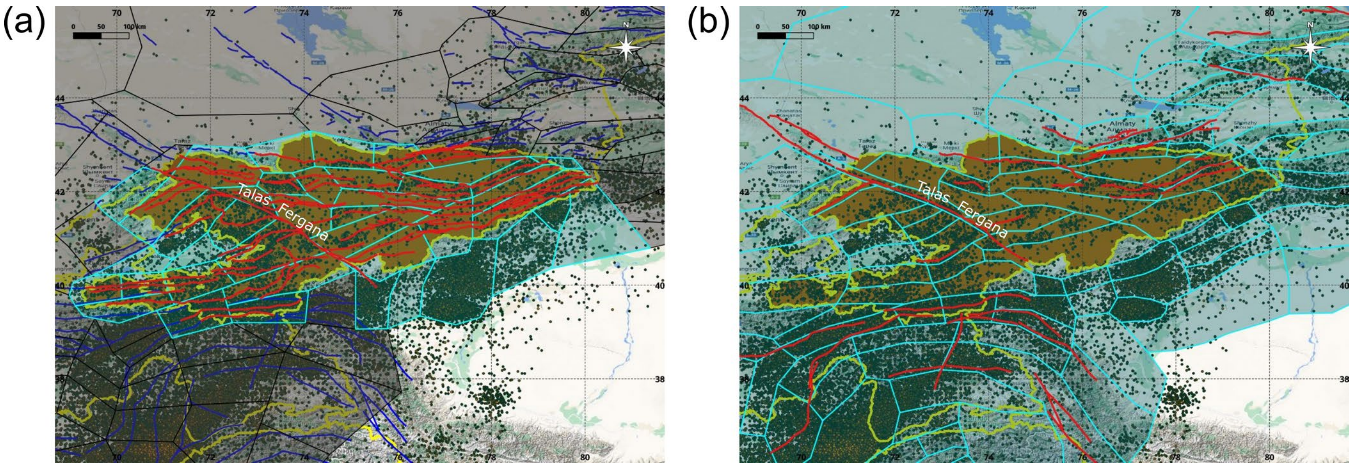

Figure 2. Fault sources and area sources shown along the earthquakes of the complete catalog (circles). The Kyrgyzstan territory is highlighted in brown. (a) Cyan area sources and red fault sources were delineated by the Kyrgyz team for their national hazard model. The rest of the merged model developed by the other teams is shown with grey area sources and blue fault sources. (b) Cyan area sources and red fault sources correspond to the alternate hazard model.

Ground motion characterization

Earthquakes occur frequently in the continental crust within Kyrgyzstan and surrounding territories. The deep earthquakes that occur under the Hindu Kush mountains [4] have a minor impact in Kyrgyzstan due to their distance (at least 150 km away from the border with Tajikistan). The ideal case would be to empirically derive region-specific GMMs. But the lack of enough strong motion data from moderate/large earthquakes in the region does not allow the development of this type of GMMs. Therefore, a set of active shallow crust GMMs derived with global databases was selected, considering their applicability to the seismic and site conditions of the region, and their ability to provide predictions for the magnitudes, distances, and periods of interest for this project.

Five GMMs were selected, which is the same set for both the national hazard model of Kyrgyzstan and the alternate model: AB10 [5], Aea14 [6], Bea14 [7], CY14 [8], and Zea16 [9]. For each model, GMM weights were selected through expert interpretation, based on the fit to the limited available observations and the trends of predictions in several scenarios. Table 1 summarizes the GMMs used in both hazard models with their respective weights. Figure 3 shows their predictions as a function of period for different magnitude and distance scenarios.

Table 1. Weights of the GMMs used in each hazard model. For each model the sum of the weights equals one.

GMM	National Model weights	Alternate Model weights
AB10	0.15	0.225
Aea14	0.2	0.225
Bea14	0.15	0.225
CY14	0.1	0.225
Zea16	0.4	0.1

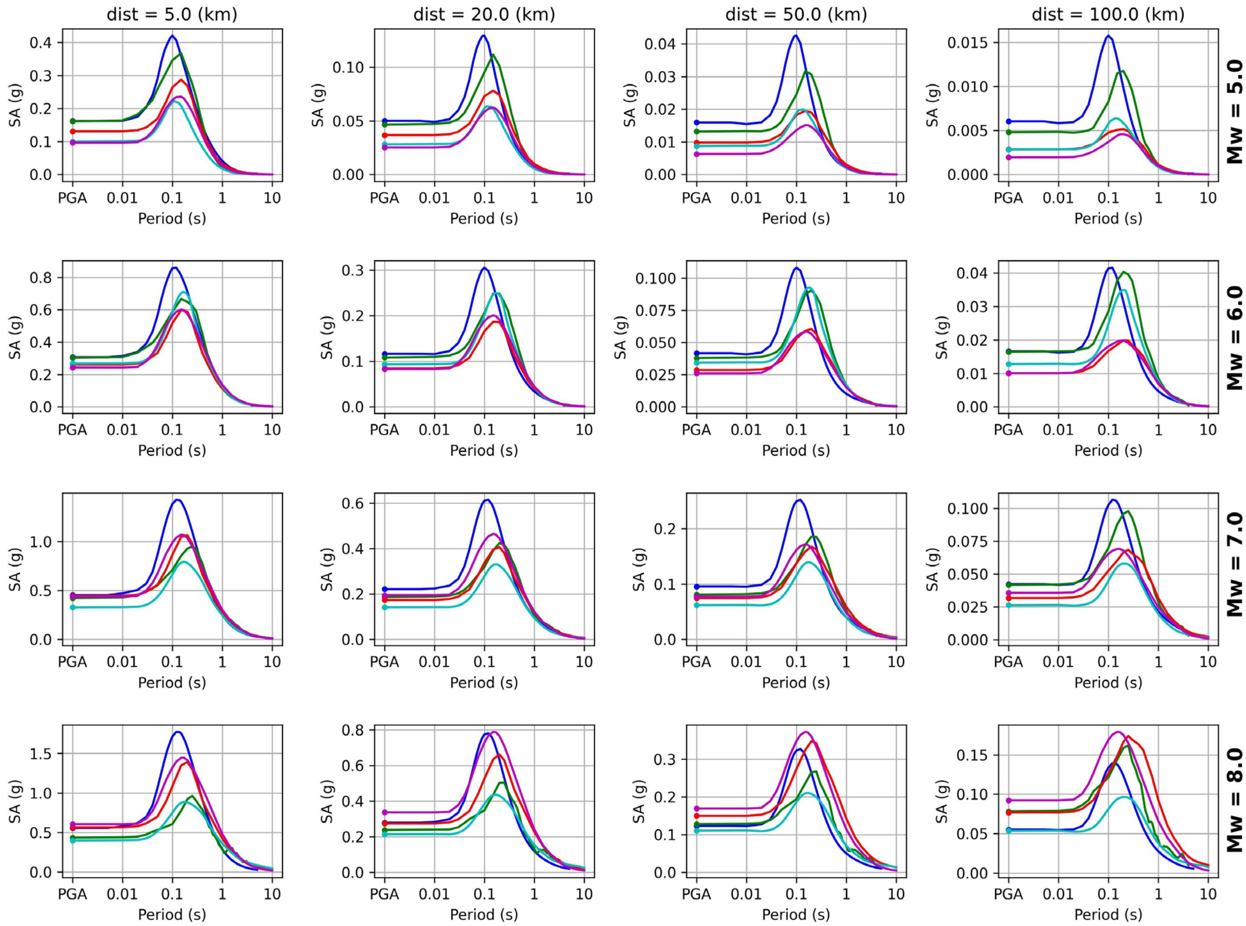

Figure 3. Set of active shallow crust GMMs used in the hazard models. Spectral acceleration (SA) predictions are shown as a function of period for different distance and magnitude scenarios. Green (AB10), red (Aea14), cyan (Bea14), magenta (CY14), and blue (Zea16).

HAZARD RESULTS

For each model, the seismic source and ground motion components were integrated and implemented as input files compatible with the OpenQuake Engine [10]. In this work, probabilistic hazard analyses were carried out using this software, which calculates different ground shaking intensity types (e.g., peak ground acceleration: PGA, and spectral acceleration as a function of period: SA(T)) for given probabilities of exceedance, among other results. PSHA results were obtained separately for each hazard model (merged and alternate) and then averaged with equal weights.

The national hazard map of Kyrgyzstan was obtained by running the PSHA for multiple locations arranged as a 5 km × 5 km grid, which is presented in Figures 4 and 5 for 2% and 10% chances of exceedance in 50 years, respectively. The first probability corresponds to a return period of 2,475 years and the latter one to a 475-year return period. The region with the largest hazard is the southwest, along the border with Tajikistan. This is the mountainous region of the northern Pamirs and the Trans-Alai range, where significant seismic activity is observed within the continental crust. Crustal seismicity in this area presents higher recurrence rates than other regions of Kyrgyzstan, resulting in higher probabilistic hazard values. Towards the center of the country, the influence of the Talas-Fergana fault in the hazard can also be observed as the spectral acceleration values are higher along its NW-SE trace, particularly at SA(0.2) and SA(1.0), where the contrast is more visible with respect to the surrounding areas (Figure 4). The regions of lower hazard are observed around the Song-Kul Lake to the northwest of Naryn city and the northern flank of the Tien Shan mountains along the border with China, due to the lower seismicity rates in these areas. The main hazard patterns are similar at a larger probability of exceedance (Figure 5), but intensity values are smaller, since they are associated with a shorter return period. In general, values of a 10% chance of exceedance in 50 years are a bit over half of the values of a 2% chance of exceedance for the same number of years.

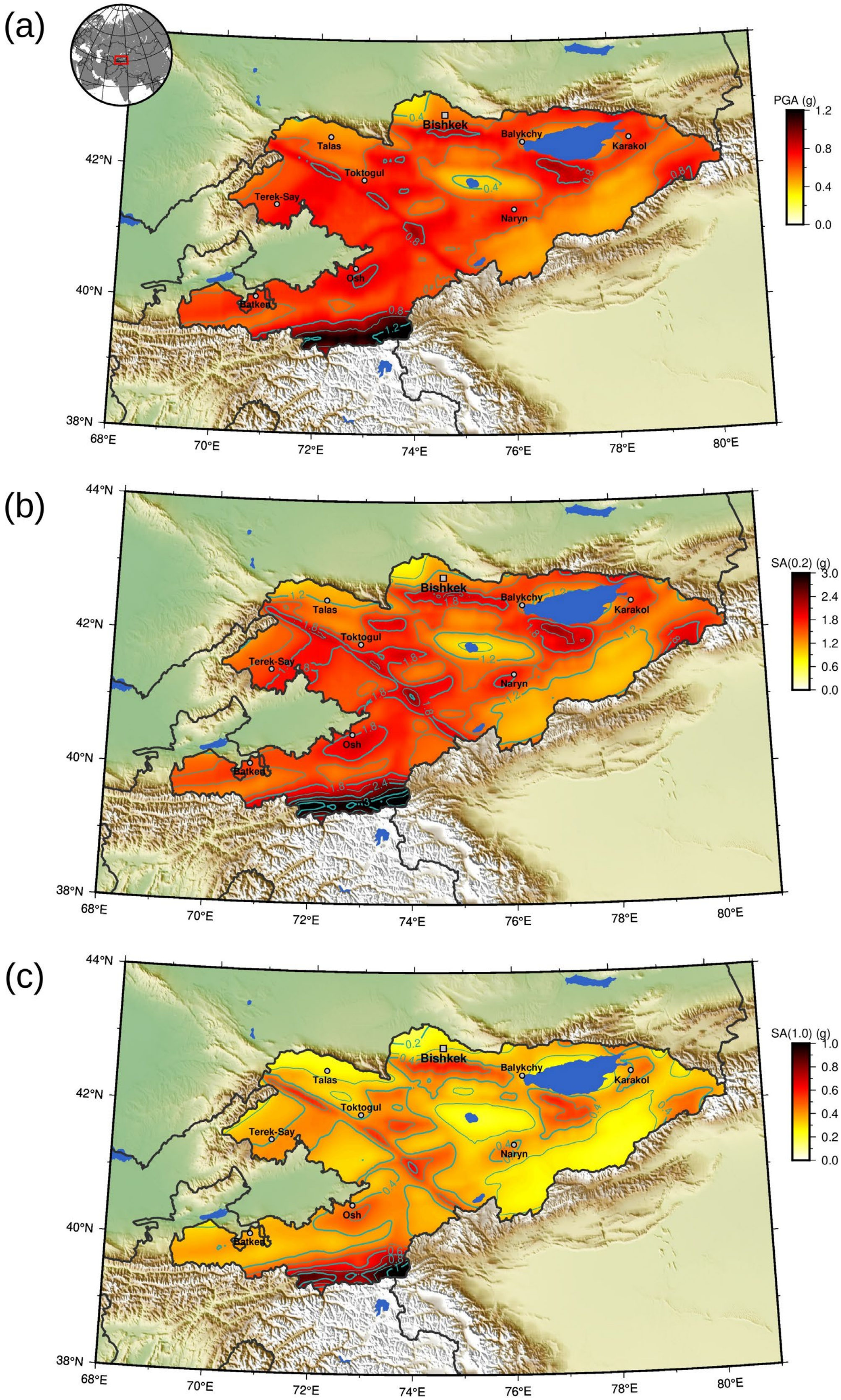

Figure 4. National hazard maps of Kyrgyzstan for a 2% chance of exceedance in 50 years. (a) PGA, (b) SA(0.2), and (c) SA(1.0).

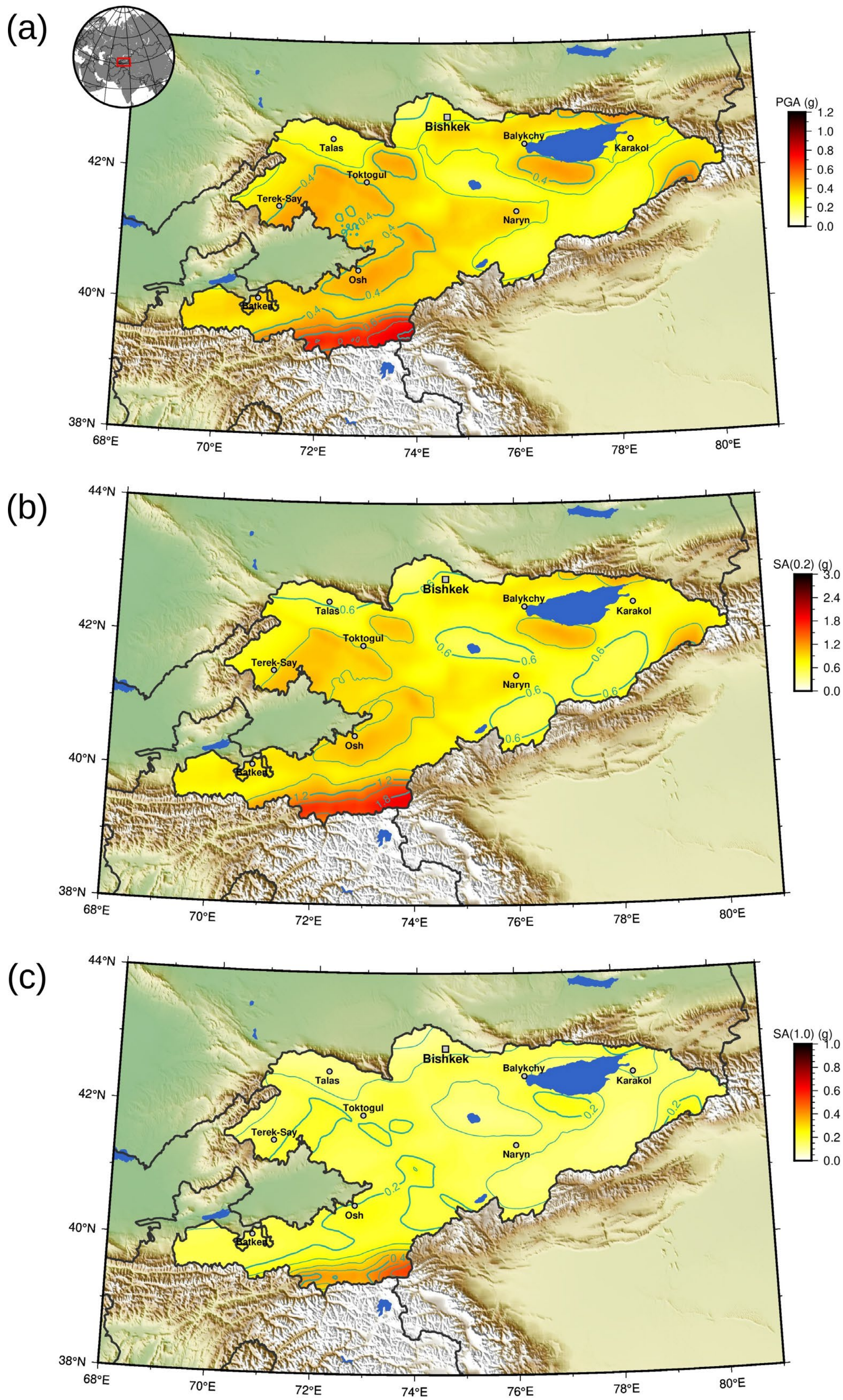

Figure 5. National hazard maps of Kyrgyzstan for a 10% chance of exceedance in 50 years. (a) PGA, (b) SA(0.2), and (c) SA(1.0). The color scale ranges are the same as those of 2% in 50 years, to highlight the contrast between these two cases.

Considering the intensity ranges observed in Kyrgyzstan, some of the major cities are located in regions of intermediate/higher hazard values. The capital Bishkek is located near the north foothills of the Kyrgyz Alatau range, close to the trace of the Chunkurchak fault. This is a region that exhibits intermediate levels of seismicity, particularly near the mountains. For a 2% chance of exceedance in 50 years, PGA is about 0.5 g and spectral accelerations can reach about 1.3 g at SA(0.2), as shown in Figure 6. Osh and Karakol cities exhibit the largest spectral accelerations among the selected cities, while Talas shows the smallest, with slightly smaller values than Bishkek.

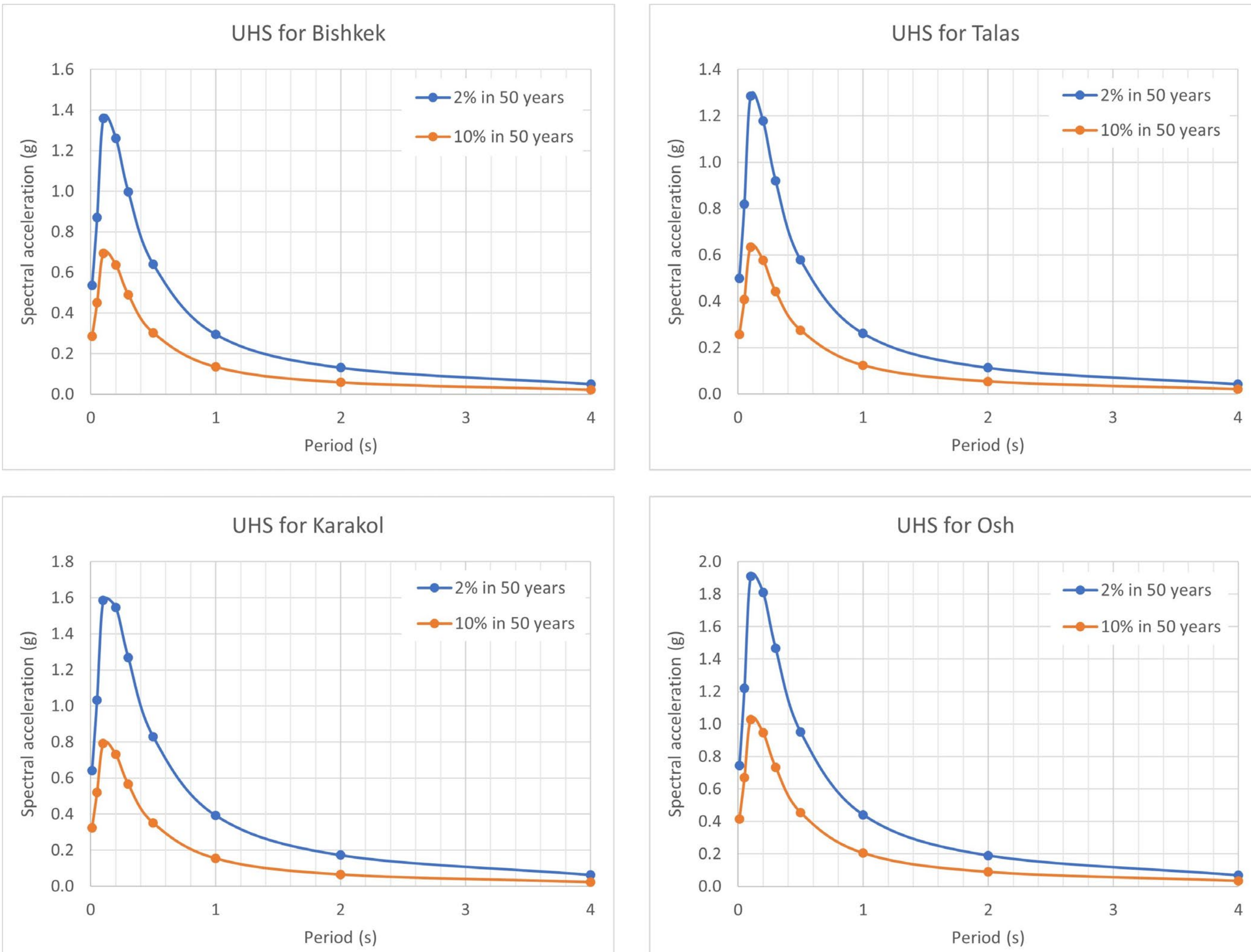

Figure 6. UHS of selected cities in Kyrgyzstan, shown for the two probabilities of exceedance analyzed in this work.

Hazard deaggregation plots show the contributions of the seismic sources based on distance and magnitude (Figure 7). In all the selected cities the hazard is contributed mainly by nearby seismic sources, i.e., within the nearest ~40 km. At larger probabilities of exceedance, the contribution from farther seismic sources slightly increases, but the difference is not significant. In Bishkek, area sources show a significant contribution to hazard in the lower magnitude range at short periods (PGA and SA(0.2)), but their contribution decreases towards longer periods (SA(1.0)), where the nearby Chunkurchak fault dominates the hazard in the larger magnitude range, with its 260 km length and its geological slip rate of 2.4 mm/yr. A similar pattern is observed in Karakol and Osh regarding the variation of area source contributions to hazard with respect to period. But in these two cities the nearby faults dominate the contribution to hazard at all periods. For the case of Karakol, the important contribution at large magnitudes is mainly associated to the nearby North Terskey Fault, which is a 170 km long fault with a slip rate of 2 mm/yr. Also, north of the city, the Tasma Fault poses an important hazard with its slip rate of 1.5 mm/yr. In Osh, the Mady Fault runs through the urban area with a measured slip rate of 0.9 mm/yr, dominating the contribution to hazard at that location. A contrasting case is Talas, where the smaller seismic occurrence rates and the small slip rates of the nearby faults (no larger than 0.2 mm/yr) resulted in smaller UHS values and a more balanced contribution to hazard between area sources and fault sources.

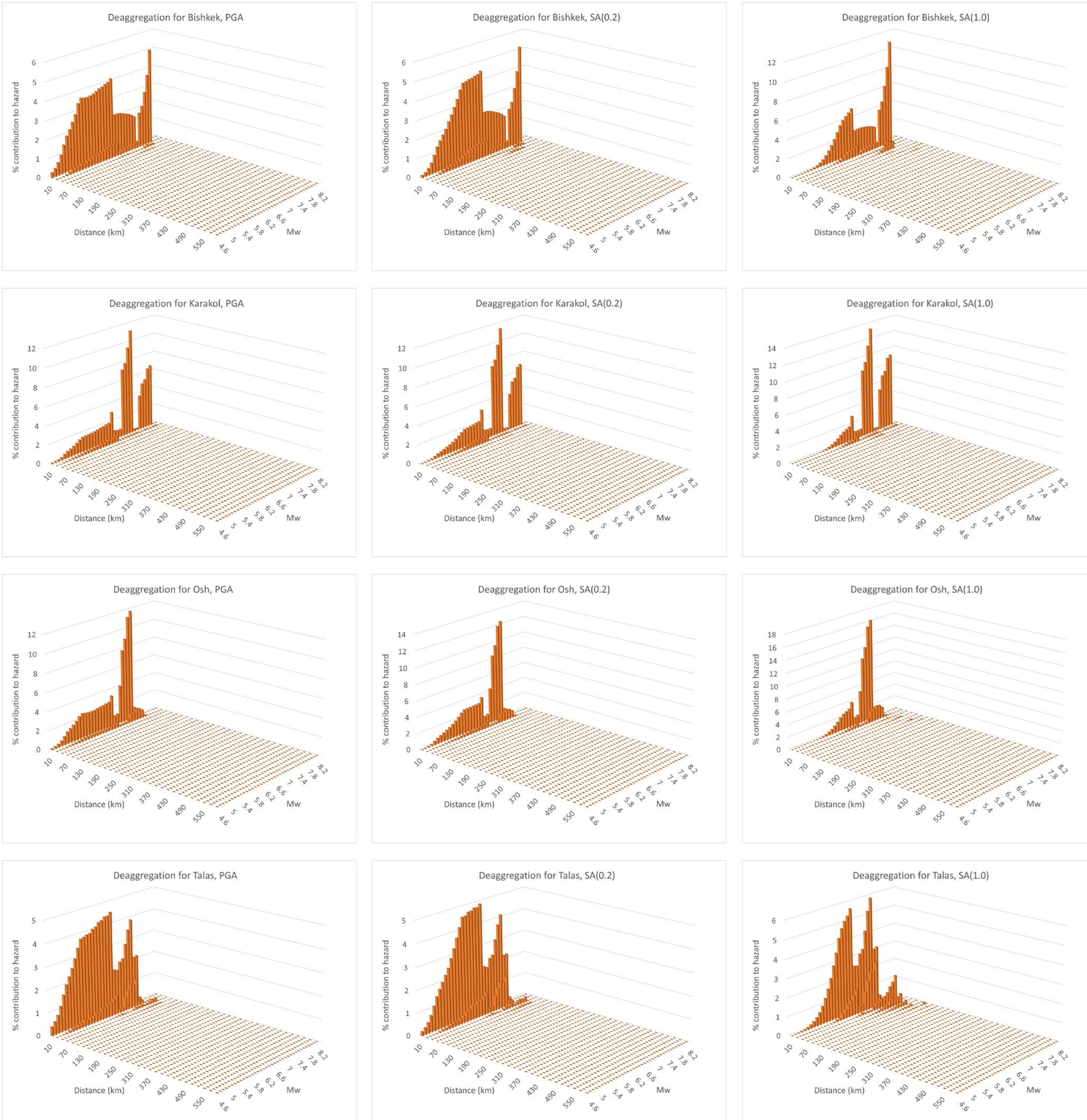

Figure 7. Hazard deaggregations for four selected cities in terms of PGA, SA(0.2), and SA(1.0) for a 2% chance of exceedance in 50 years.

CONCLUSIONS

The recently published earthquake catalogue for Central Asia with a significant increase of earthquake detections, as well as the detailed fault characterization work by local teams, allowed the possibility of developing a new generation of seismic hazard models for probabilistic seismic hazard analyses in Kyrgyzstan, Kazakhstan, and Tajikistan.

This work presents PSHA results in Kyrgyzstan. PGA and SA(T) values vary significantly within the territory, highly influenced by local seismic sources within the continental crust. The mountainous region along the border with Tajikistan exhibits the highest hazard in the country. However, the main cities in Kyrgyzstan are relatively far from that region. The assessment of selected cities shows an important contribution to hazard of nearby seismic sources (within 40 km), which is typical of active crustal tectonic regimes. When faults are significantly active (large slip rates), they usually dominate the contribution to hazard near them at large magnitudes. Area sources usually account for smaller-magnitude seismicity, and their contribution to hazard is more prominent at short periods. The four analyzed cities show important contributions of both types of sources. But the faults near Karakol, and Osh pose the largest hazard to population at those locations.

These new hazard models developed with an enhanced and richer seismotectonic database are an important improvement for PSHA in the region. The PSHA results from these models will be essential to improve site hazard assessments, as well as for future building code updates, which can include guidelines for different intensity types and probabilities of exceedance.

ACKNOWLEDGMENTS

This work was performed under the auspices of the United States Department of Energy by Lawrence Livermore National Laboratory under contract DE-AC52-07NA27344. We thank Kanatbek Abdrakhmatov and Alexandra Frolova from the National Academy of Science of Kyrgyz Republic for contributing geologic information of faults, as well as earthquake data from the Kyrgyzstan archives. Maps were created using QGIS and Generic Mapping Tools [11].

REFERENCES

[1] Bondár, I., and Storchak, D. (2011). Improved location procedures at the International Seismological Centre. *Geophysical Journal International*, *186*(3), 1220-1244. https://doi.org/10.1111/j.1365-246X.2011.05107.x

[2] Onur, T., Gok, R., Mackey, K., Abrams, K., Berezina, A., Mikhailova, N., Bekturganova, B., Murodkulov, S., Bondar, I., and Herrera, C. (2021). Central Asia Seismic Hazard Assessment (CASHA) "Complete" catalog of earthquakes. *Lawrence Livermore National Laboratory (LLNL). Report LLNL-TR-828313*. https://doi.org/10.2172/1827508

[3] International Seismological Centre (2023), On-line Bulletin, https://doi.org/10.31905/D808B830

[4] Kufner, S. K., Schurr, B., Sippl, C., Yuan, X., Ratschbacher, L., Akbar, A. M., Ischuk, A., Murodkulov, S., Schneider, F., Mechie, J., and Tilmann, F. (2016). Deep India meets deep Asia: Lithospheric indentation, delamination and break-off under Pamir and Hindu Kush (Central Asia). *Earth and Planetary Science Letters*, 435, 171-184. https://doi.org/10.1016/j.epsl.2015.11.046

[5] Akkar, S., and Bommer, J. J. (2010). Empirical equations for the prediction of PGA, PGV, and spectral accelerations in Europe, the Mediterranean region, and the Middle East. *Seismological Research Letters*, *81*(2), 195-206. https://doi.org/10.1785/gssrl.81.2.195

[6] Abrahamson, N. A., Silva, W. J., and Kamai, R. (2014). Summary of the ASK14 ground motion relation for active crustal regions. *Earthquake Spectra*, *30*(3), 1025-1055. https://doi.org/10.1193/070913EQS198M

[7] Boore, D. M., Stewart, J. P., Seyhan, E., and Atkinson, G. M. (2014). NGA-West2 equations for predicting PGA, PGV, and 5% damped PSA for shallow crustal earthquakes. *Earthquake Spectra*, *30*(3), 1057-1085. https://doi.org/10.1193/070113EQS184M

[8] Chiou, B. S. J., and Youngs, R. R. (2014). Update of the Chiou and Youngs NGA model for the average horizontal component of peak ground motion and response spectra. *Earthquake Spectra*, *30*(3), 1117-1153. https://doi.org/10.1193/072813EQS219M

[9] Zhao, J. X., Zhou, S., Zhou, J., Zhao, C., Zhang, H., Zhang, Y., Gao, P., Lan, X., Rhoades, D., Fukushima, Y., Somerville, P. G., and Irikura, K. (2016). Ground-motion prediction equations for shallow crustal and upper-mantle earthquakes in Japan using site class and simple geometric attenuation functions. *Bulletin of the Seismological Society of America*, *106*(4), 1552-1569. https://doi.org/10.1785/0120150063

[10] Pagani, M., Monelli, D., Weatherill, G., Danciu, L., Crowley, H., Silva, V., Henshaw, P., Butler, L., Nastasi, M., Panzeri, L., Simionato, M., and Vigano, D. (2014). OpenQuake engine: An open hazard (and risk) software for the global earthquake model. *Seismological Research Letters*, 85(3), 692-702. https://doi.org/10.1785/0220130087

[11] Wessel, P., Luis, J. F., Uieda, L., Scharroo, R., Wobbe, F., Smith, W. H., & Tian, D. (2019). The generic mapping tools version 6. *Geochemistry, Geophysics, Geosystems*, *20*(11), 5556-5564. https://doi.org/10.1029/2019GC008515